IEEE Access
Multidisciplinary | Rapid Review | Open Access Journal

Received August 29, 2019, accepted September 13, 2019, date of publication September 18, 2019, date of current version October 3, 2019.

Digital Object Identifier 10.1109/ACCESS.2019.2942215

A Neural Network Processing Method Based on Self-Assembly Equipment for Optical Image Display Standardization

ZILONG LIU[1], YIQIN JIANG[1], YUXIAO LI[1], JIN LI[2], ZHUORAN LI[1], SHUGUO ZHANG[3], YUSHENG LIAN[4], AND RUPING LIU[4]

[1]Optic Division, National Institute of Metrology, Beijing 100029, China
[2]Photonics and Sensors Group, Department of Engineering, University of Cambridge, Cambridge CB3 0FA, U.K.
[3]State Grid Beijing Electric Power Company Training Center, Beijing 100041, China
[4]School of Printing and Packaging Engineering, Beijing Institute of Graphic Communication, Beijing 102600, China

Corresponding author: Jin Li (jl918@cam.ac.uk)

This work was supported in part by the National Natural Science Foundation of China (NSFC) under Grant 61875180 and Grant 61605012, in part by the National Key Research and Development Program of China under Grant 2017YFF0205103, in part by the Beijing Natural Science Foundation under Grant 2162017, and in part by the Beijing Municipal Science and Technology Commission under Grant Z181100004418004.

ABSTRACT Optical image is a kind of important data for communication because it is a two or three -dimensions data set to express communication information such as geographical signal, medical signal, remote sensing signal, etc. Thus, how to express the optical image properly is critical for the communication analytics. A new display method for optical image is described which is derived from the concept-Grayscale Standard Display Function (GSDF) which has been defined in DICOM, a medical image standard. The method analysis GSDF based on neural network processing which is different to DICOM. And the training data are from a self-assembly Equipment in NIM which is a traceable optical display equipment. Thus, the method has common usage for all optical image display, exceeding medical image. Furthermore, it is suitable for standardization because of the traceability.

INDEX TERMS Optical image display Grayscale Standard Display Function (GSDF) neural network standardization.

I. INTRODUCTION

According to the communication technology development, the signal is extended from one dimension to high dimension, so image as a multi-dimension data is suitable to express the communication data, especially optical image is used more widely for visual usage [1]–[4]. But affected by the difference in performance of display devices and the environment, the same image will exhibit different visual characteristics on different display devices, which interferes with the interpretation of the images [5]–[7]. Different display effects may lead to misdiagnosis and potential safety hazards, especially in industries requiring results identification, such as medical imaging, non-destructive flaw detection imaging, etc. [5], [6], [8]. Therefore, it is necessary to propose and implement a display standard.

The Grayscale Standard Display Function (GSDF) which is defined in Digital Imaging and Communications in Medicine (DICOM, a medical image standard, published by ACR-NEMA, a joint committee of the American College of Radiology and the National Electrical Manufacturers Association [9]) provides a solution by mapping the grayscale to an objective quantitative mechanism of a given luminance range. Specifically, the function establishes the relationship between grayscale and luminance, providing a standardized display specification for grayscale images. Existing GSDF in DICOM is currently widely used to calibrate medical image display and printing devices as a display specification [10], [11]. Based on the nonlinear perceptual visual characteristics of human eyes, a compromised GSDF with a brightness of 0.05 cd/m^2-4000 cd/m^2 is given in the form of a higher-order logarithmic expression, taking the image display characteristics in different luminance ranges into account.

The existing GSDF in DICOM is limited for medical image. It is not common for other application [12], [13]. Therefore, a common method of GSDF for all optical image is needed, so a backpropagation neural network (BPNN) method of GSDF based on a traceable measurement

The associate editor coordinating the review of this manuscript and approving it for publication was Valentina E. Balas.

This work is licensed under a Creative Commons Attribution 4.0 License. For more information, see http://creativecommons.org/licenses/by/4.0/

equipment is established for common usage. We experimented on a self-assembly grayscale standard display equipment to obtain experimental data of high luminance range as a neural network data set. Then a GSDF neural network model is established by an optimized BP neural network algorithm, of which the luminance range is 0.80 cd/^{2}-5000 cd/m^2 as the calculation mean square error (MSE) of the normalized data is smaller than 10^{-3}. It can provide a standardized display specification for more grayscale images. Especially, the DLP technology is used to established the experiment equipment. As DLP is a digital technology, and GSDF is a property of grayscale which is a discrete parameter, so a digital technology is suitable to realize the discrete property. That means the experiment data has the lowest uncertainty.

II. METHOD

Based on the human eye's nonlinear perceptual visual characteristics of nonlinear variation of contrast sensitivity in bright and dark fields, the Barten model that achieves linear perception in the overall range was chosen to calculate contrast sensitivity in DICOM 3.14. A composite function between contrast sensitivity and luminance L, spatial frequency u, and visual angle is established in the Barten model that can be described as [14]

$$S(u) = \frac{1}{k}\sqrt{\frac{T}{2}}\frac{M_{opt}(u)}{\sqrt{(\frac{1}{\eta pI}+\frac{\Phi_0}{(1-F(u))^2}+\Phi_{ext}(u))(\frac{1}{X_0^2}+\frac{1}{X_E^2}+(\frac{u}{N_E})^2)}} \tag{1}$$

where the optical transfer function based on Gaussian point-spread function is defined by [15]

$$M_{opt}(u) = e^{-\pi^2\sigma^2u^2} \tag{2}$$

where σ is the radial standard deviation of the point-spread function. d is the pupil diameter of the human eye, which can be expressed as [16]

$$\sigma = \sqrt{\sigma_0^2 + (C_{sph}{*}d^3)^2} \tag{3}$$

$$d = 4.6 - 2.8\tanh(0.4\log_{10}(0.625L)) \tag{4}$$

where L is the luminance of an object. In a state consistent with the nonlinear perception characteristics of human eyes', it is found that the system characteristic curve shows an obvious logarithmic characteristic for a simple image with a narrow luminance range, as well as a strongly-bent characteristic for a complex image with a wide luminance range. To fit the curves of both features, the high-order logarithmic structure is chosen as the function structure in DICOM. The GSDF with a luminance range of 0.05cd/m^2-4000cd/m^2 is represented by [4]

$$\log_{10}L(j) = \frac{a + c\ln(j) + e(\ln(j))^2 + g(\ln(j))^3 + m(\ln(j))^4}{1 + b\ln(j) + d(\ln(j))^2 + f(\ln(j))^3 + h(\ln(j))^4 + k(\ln(j))^5} \tag{5}$$

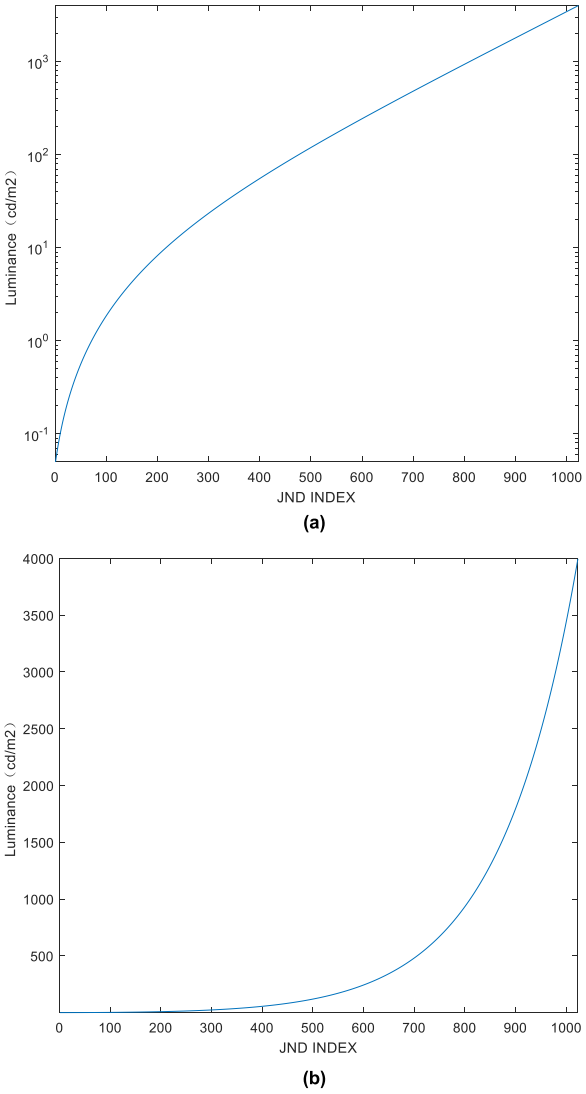

FIGURE 1. GSDF curve in DICOM in two coordinates. (a) Curve in logarithmic coordinates, (b) curve in linear coordinates.

$$j(L) = A + B\log_{10}(L) + C(\log_{10}(L))^2 + D(\log_{10}(L))^3 + E(\log_{10}(L))^4 + F(\log_{10}(L))^5 + G(\log_{10}(L))^6 + H(\log_{10}(L))^7 + I(\log_{10}(L))^8 \tag{6}$$

where j represents the just noticeable difference, while L is the corresponding luminance. Other parameters in Eqs. (5) and (6) are constant coefficients. The GSDF curve in logarithmic coordinates is shown in Fig.1(a). Since the subsequent experimental data is plotted in linear coordinates, we convert it to linear coordinates as shown in Fig.1(b).

It is proposed that a GSDF with monotonic continuity and a single expression in the luminance range of 0.05cd/m^2-4000cd/m^2 in the DICOM standard. It can be seen that there are certain limitations. 1)As the receiving terminal of the image is replaced by the detector, the distinguishable luminance area is greatly increased, which means that the

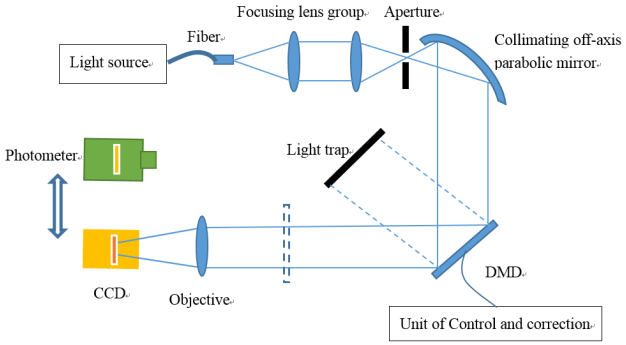

FIGURE 2. Schematic diagram of digital grayscale generation equipment (DGGE).

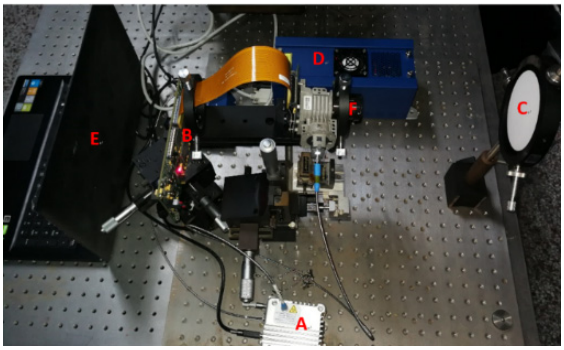

FIGURE 3. Self-assembly digital grayscale generation equipment (DGGE).

upper limit of the display luminance exceeds 4000cd/m^2; 2) there is no traceability analysis on measurement devices and methods; 3)It is described by the traditional mathematical expression of a single structure in the whole luminance area, which increases the visual error of nonlinear perception to some extent.

To solve these problems, a neural network processing method is established. The key of this method is the training data. A digital grayscale generation equipment named DGGE is established to provide the training data for the BPNN method. DGGE used digital light process (DLP) technology to match the GSDF digital level as shown in Fig.2. Every department of DGGE including light source, detector, DMD(Digital Micromirror Device) controller, optics components can be calibrated by corresponding references in NIM(National Institute of Metrology, China), so the training data from DGGE is precise and common. That means the method is suitable for different image calibration and image display standardization.

Fig.3 is the photograph of DGGE. In the photo, A is a light source module EQ-99XFC LDLS(Laser Driven Light Source) which is made by the ENERGETIC company, with characteristics of high brightness and wide bandwidth is adapted to provide incident light. Its' output luminance is up to 5000cd/m^2 and the laser excitation mode ensures its' stability as well. B is a digital light processing module including DMD, drive and control circuits, projection lens, etc.

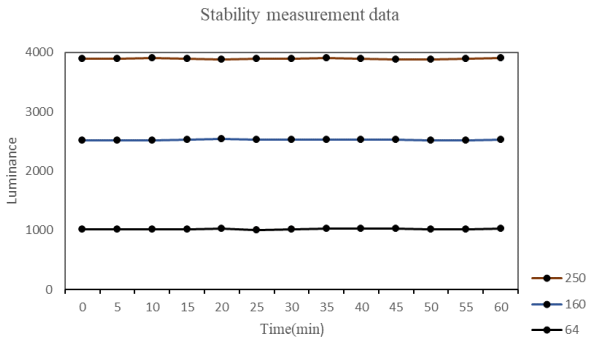

FIGURE 4. Experimental data for stability measurement ay 250th, 160th, 64th *DDLs*.

As for the DMD, we select model DLP-7000 made from Texas Instruments, which has an output precision of up to 16 bits. C is a Luminance screen, a white polyester fluoroethylene-coated whiteboard with a diameter of 100mm and a diffuse reflectance of 97%. D is a DC power supply, and the constant current working model is used in the device. E is a laptop for DLP control and data processing. Besides, we choose Photo Research's PR655 model photometer (not labeled in Fig.3) to measure the luminance value of the terminal output.

The high-intensity light enters the digital light processing module through the fiber-coupled output and is displayed with different luminance after being adjusted by the DMD. The light is received by the luminance screen and measured with a photometer.

III. ANALYSIS

The relative uncertainty of the grayscale change given by DGGE is analyzed. The relevant data results are calculated at 8-bit input accuracy with the luminance range of 0.80 cd/m^2-4000 cd/m^2.

A. THE UNCERTAINTY OF THE LIGHT SOURCE STABILITY

The uncertainty of the light source stability is the major source. The light source operates in a constant current mode according to the digital control mode of the device. And the grayscale is created by the DDL(Digital Driven Level) of DMD. Three DDLs of 250, 160, 64are selected to measure the luminance of the screen in one hour with 5 minutes' interval. Fig.4 shows that the source stability tends to decrease as the DDL (equal gray level) increases. Taking the experimental data at the 250th level, the uncertainty introduced by source stability calculated by the Bessel formula is

$$u(S_s) = \sqrt{\frac{\sum_{i=1}^{n} (L_i - \overline{L})^2}{n-1}} = 0.08\% \tag{7}$$

where n indicates the number of measurements.

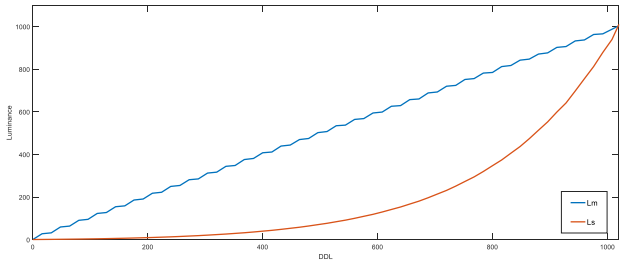

FIGURE 5. System characteristic curve obtained by measurement Lm and calculated characteristic curve conforming to human visual characteristics L_s.

B. THE UNCERTAINTY INTRODUCED BY DIGITAL CONTROL IS THE OTHER SOURCE

DMD is a digital device controlled by Field Programmable Gate Array (FPGA), which indicates that its accuracy and repeatability are not uncertain. We take the uncertainty component as 0.1% for convenience of calculation, that is, there is one exception in the results of 1000 runs. Consequently, the relative uncertainty of the device in the measurement process can be described as

$$u(L_m)/L_m = \sqrt{u^2(S_s) + u^2(e)} = 0.13\% \tag{8}$$

Additionally, the uncertainty of the photometer measurement is given by the calibration certificate of NIM, and the standard uncertainty is 1%.

IV. EXPERIMENT

Specifically, the experimental process includes the following 3 steps.

Firstly, we measured the system characteristic curve over a suitable luminance range of 0.96 cd/m^2-1003.14 cd/m^2, by which a 12.5% attenuator is added to the system. Available data indicates that the maximum and minimum luminance ratio that can be resolved by the human eye is approximately 1000:1 at an environment of usual luminance and that the most perceptually sensitive luminance for human eyes is around 1000 cd/m^2 [19]. After warming up the device for about 15 minutes, we enter the DDL in the order of decreasing steps from 255 to 0 with 8-bit precision. The measurement results are shown as in Fig.5.

Secondly, we built a look-up table between the theoretical DDL and input DDL with different precision. The Barten model has been proven by existing experiments to achieve good contrast balance and similarity for simple images and most complex images [17]. Under a test condition with a viewing distance of 250 mm, a 2deg × 2deg square sinusoidal raster image has a size of about 8.7mm × 8.7mm, and the spatial frequency equals about 0.92 line pairs per millimeter. Equation (1) can be simplified as

$$S(L) = \frac{q_1 M_{opt}(L)}{\sqrt{\frac{q_2}{d^2 L} + q_3}} \tag{9}$$

with $q_1 = 0.1183, q_2 = 3.9628{*}10^{-5}, q_3 = 1.3562{*}10^{-7}$.

TABLE 1. Standard luminance (L_s) and measured luminance (L_m) corresponding to some typical DDL_s.

DDL	24	72	124	152
L_s(cd/m^2)	1.25	18.07	69.66	131.02
L_m(cd/m^2)	31.94	285.06	502.26	598.8

DDL	184	212	236	255
L_s(cd/m^2)	258.66	458.44	740.81	1003.14
L_m(cd/m^2)	723.96	842.41	932.66	1003.18

Just noticeable difference (JND) is defined as the smallest difference in stimuli that can cause differential perception in Psychophysics [18]. As a consequence just noticeable luminance (JNL) can be defined as the minimum amount of luminance difference caused differential perception. The mean luminance of the next higher level is calculated by adding the peak-to-peak modulation to the mean luminance of the previous level:

$$L_{j+1} = L_j \frac{1 + S_j}{1 - S_j} \tag{10}$$

where S_j indicates the contrast sensitivity calculated from the Barten model. In Fig. 5, L_s represents the ideal output according to the Equation (10). The experimental data L_m and calculation data L_s corresponding to several typical DDLs are shown in Table 1. Therefore, a look-up table of the standard DDL-input DDL is obtained, that is, when the input is pressed according to the table, it can be considered that the display luminance is in conformity with the visual characteristics of the human eye. Similarly, cubic spline interpolation is used to get a lookup table with 10-bit accuracy.

Lastly, the attenuator is removed from DGGE and new data in high luminance range are measured. Turn off the illumination source to keep the ambient luminance as low as possible. Then input DDL 1023 after preheating the device with 10-bit precision. Accordingly, the lowest and highest luminance measured by the photometer is 0.80 cd/m^2, 5000.0 cd/m^2. We input the DDL in order from highest to lowest according to the look-up table. Thus 1024 sets of data are obtained as a neural network data set.

V. RESULT

As mentioned above, it is a model of high-order logarithm being used to describe the GSDF in the luminance range of 0.05 cd/m^2-4000 cd/m^2 in DICOM. And further expansion of the luminance range will increase the computational complexity and reduce data convergence, which makes it difficult to choose a reasonable function structure. That is, it is not feasible to use a traditional expression to describe the nonlinear relationship between the DDL and the luminance over the entire region of interest.

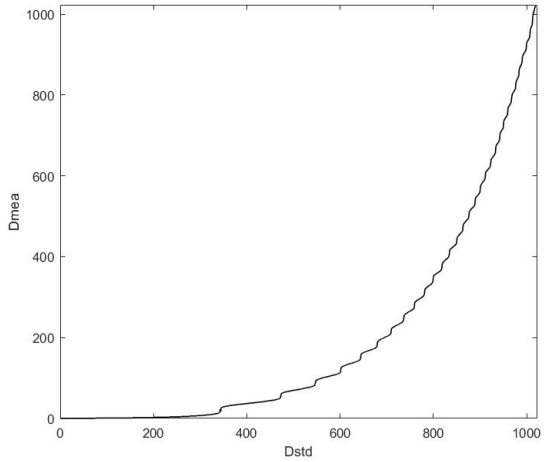

FIGURE 6. A 10-bit precision lookup table for standard DDL (Dstd)–measured DDL (Dmea) by cubic spline interpolation.

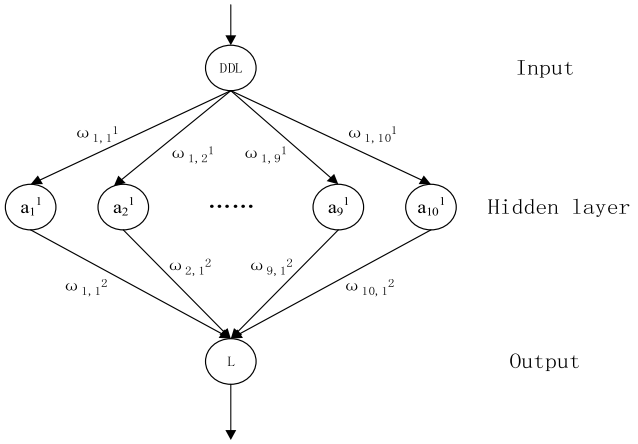

FIGURE 7. 3-layer neural network topology–input layer with 1 neurons (DDL), output layer with 1 neurons (L), and a hidden layer with 10 neurons included.

The BP neural network algorithm is chosen to solve the GSDF in this paper. BP neural network is a multi-layer intelligent algorithm based on the principle of error back propagation, which can fully approximate arbitrarily complex nonlinear relations [19]. It consists of several neurons with the same nonlinear characteristics, which form the input, hidden and output layers. The neural network model can be trained by given input and output data, and be described as a set of available weights and thresholds after it is parameterized. BP neural network has a high degree of nonlinearity and strong generalization, which solves the problem of poor convergence and low fitting of traditional function expressions. To analyze the GSDF in the luminance range of 0.80cd/m^2-5000cd/m^2, the DDL is used as the input layer, and the corresponding luminance is used as the output layer, according to the 1024 sets of experimental data obtained above.

First of all, a 3-layer network structure is selected to establish an initial hierarchical mapping model. As shown in Fig.7, the number of neurons in the input layer DDL, hidden layer,

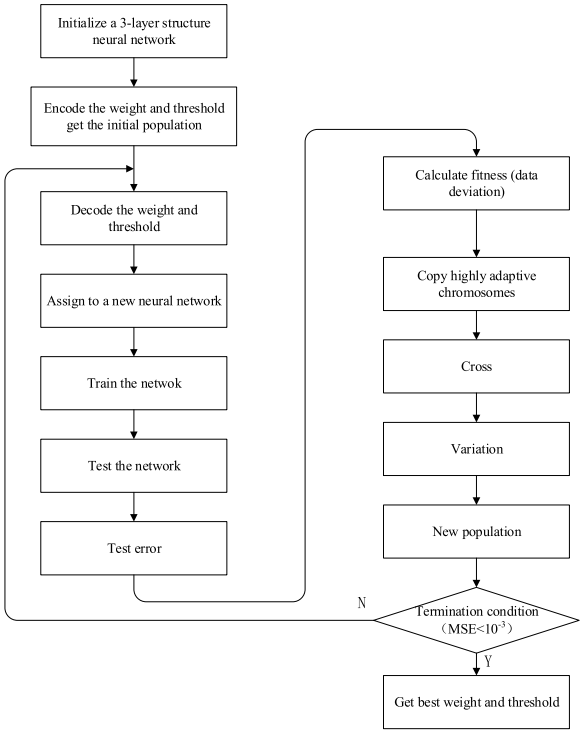

FIGURE 8. Flow chart of BP neural network algorithm optimized by genetic algorithm. The condition that the genetic algorithm terminates the iterative operation is that the MSE of the normalized data is less than 10^{-3}, and the weights and thresholds of the neural network are obtained.

and output layer L is set to 1, 10, and 1, respectively. The weight of information transmitted between neurons is $\omega_{i,j}^N$, indicating the weight information from the i_{th} neuron of the $(N-1)_{th}$ layer to the j_{th} neuron of the N_{th} layer. b_j^N represents the threshold of the j_{th} neuron in the N_{th} layer, and the output information of the j_{th} neuron in the Nth layer can be described as

$$a_j^N = s(\sum_i \omega_{i,j}^N a_i^{N-1} - b_j^N) \tag{11}$$

where s is the activiation function to establish a nonlinear map, and the sigmoid function $s(u) = 1/(1+e^{-u})$ is selected in this paper.

For the neural network dataset, 70%, 10% and the remaining 20% of the experimental data are selected as the training, validating and test data sets respectively; So we get an initialized neural network model with the Levenberg-Marquardt algorithm as the training function.

Sometimes BP neural network has disadvantages of falling into local minimum and poor global search ability [20]–[22]. In this paper, the genetic algorithm is used to optimize it, which is of help to solve the optimal weights and thresholds of the neural network in a global scope. The genetic algorithm searches for global optimal solutions by imitating natural selection and genetic mechanisms [23]. It has good convergence and global search ability with low computation time and high robustness, which makes up for the shortcomings of the BP neural network algorithm. The fitness of the

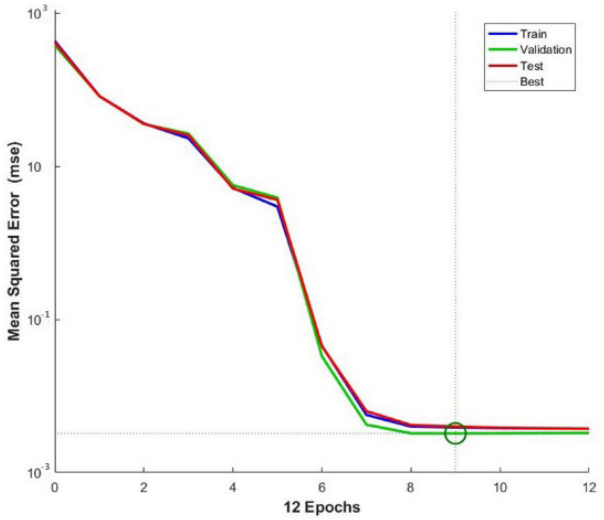

FIGURE 9. MSE of 9 iterations. The preset termination condition was met at the 9th time.

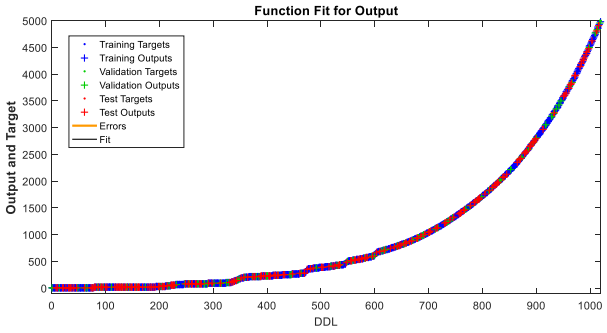

FIGURE 10. Output by simulation corresponding to the 0-1023 DDLs.

optimization process is set to the absolute deviation of the simulation results of a neural network model from the target. Chromosomes with high fitness (small absolute deviation) are copied, crossed, and variated through multiple iterations until the termination condition is reached, that is, the MSE of the normalized data is less than 10^{-3}.

The optimal weights and thresholds in the global scope are obtained after 9 iterations. We reshaped the neural network model with these parameters. At a 10-bit precision, the luminance (Output) corresponding to the DDL of 0-1023 is obtained through the simulation. The calculation error and regression coefficient of the output of the model are shown in the Fig.11 and Fig.12.

VI. DISCUSSION

In summary, by using an optimized BP neural network algorithm, we established a neural network model of GSDF with a luminance range of 0.80 cd/m^2-5000 cd/m^2, of which the topology is a 3-layers' structure and the MSE of the normalized data is less than 10^{-3}. Experiments are conducted on a self-assembly grayscale equipment DGGE with a relative uncertainty of 0.13%, which ensures the reliability of the target data. The DDL is used as input and the output is the

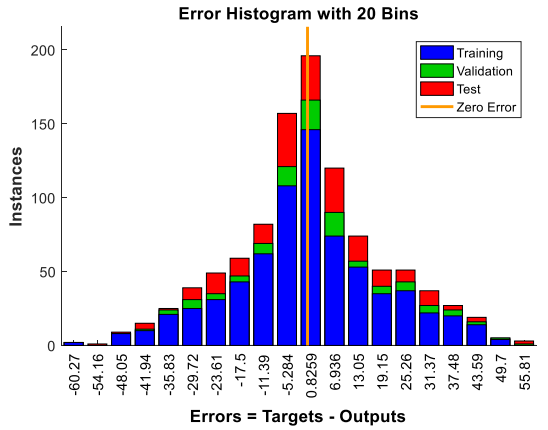

FIGURE 11. Histogram of error (target value minus simulation output).

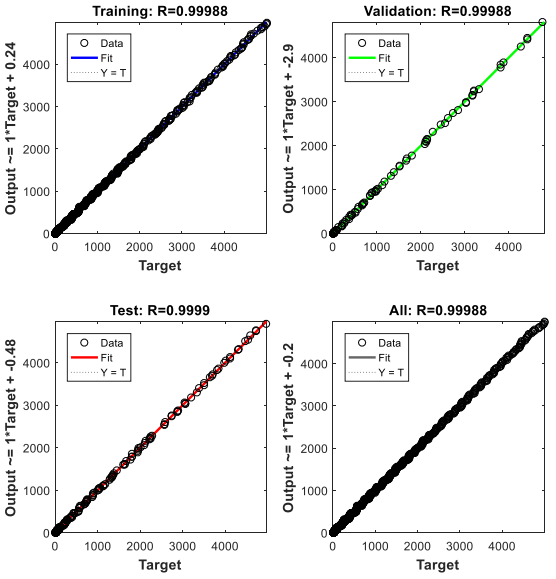

FIGURE 12. Regression coefficient of each data set. (a) Training dataset, (b) validation dataset, (c) test dataset, (d) all of the data.

TABLE 2. Simulation outputs and targets corresponding to some typical levels.

DDL	Output(cd/m^2)	Target(cd/ m^2)	Error
16	0.96	0.92	0.04
128	17.28	15.99	1.29
236	84.09	80.51	3.58
340	127.21	129.83	-2.62
452	262.43	268.76	-6.33
568	532.99	528.84	4.15
672	902.82	895.31	7.51
798	1692.16	1681.48	10.68
886	2561.09	2570.05	-8.96
954	3626.38	3636.12	-9.74
1023	5011.26	4998.59	12.67

corresponding luminance. The standardized display requirements of images with different resolutions can be met by setting different input precisions, and this paper takes 10bit as an example.

Theoretically, any monotonous continuous function on the region of interest can achieve display standardization. We achieve several extra goals. Firstly, replacing traditional function expressions with neural network models can effectively reduce regression errors. Secondly, the standard data is obtained on self-assembly equipment based on DLP technology, which ensures that such measurement method is traceable. Besides, the human visual property is retained to the utmost in this model.

Compared with the existing GSDF in DICOM, it avoids the error introduced by complex mathematical expressions and expands the range of grayscale. Thus, a neural network model of GSDF provides a solution for image normalization with higher resolution and wider grayscale range.

VII. CONCLUSION

A neural network processing method for optical image display is described based on the training data deriving from a self- assembly Equipment DGGE in NIM, which is traceable and common. Not only for medical images, but the standardized display of grayscale images is also necessary for remote sensing, security, industrial inspection, and the model can be easily applied to other fields. The luminance range can be further extended by changing the photometer with a wider measuring range. By setting different input precisions for the model, the required luminance output can be obtained, thus achieving the standard display of grayscale images. In addition, for display devices with different luminance ranges, we can also calibrate them based on this method. And it is suitable for standardization because of the traceability.

ACKNOWLEDGMENT

The authors declare no conflict of interest.

REFERENCES

[1] *Digital Imaging and Communications in Medicine (DICOM)PS3*, Nat. Elect. Manufacturers Assoc., Rosslyn, VI, USA, 2009.
[2] J. Li, Y. Fu, G. Li, and Z. Liu, "Remote sensing image compression in visible/near-infrared range using heterogeneous compressive sensing," *IEEE J. Sel. Topics Appl. Earth Observ. Remote Sens.*, vol. 11, no. 12, pp. 4932–4938, Dec. 2018.
[3] J. Li and Z. Liu, "Optical focal plane based on MEMS light lead-in for geometric camera calibration," *Microsyst. Nanoeng.*, vol. 3, Nov. 2017, Art. no. 17058.
[4] J. Li, Z. Liu, and F. Liu, "Using sub-resolution features for self-compensation of the modulation transfer function in remote sensing," *Opt. Express*, vol. 25, no. 4, pp. 4018–4037, 2017.
[5] E. Seto, A. Ursani, J. A. Cafazzo, P. G. Rossos, and A. C. Easty, "Image quality assurance of soft copy display systems," *J. Digit. Imag.*, vol. 18, no. 4, pp. 280–286, Jan. 2005.
[6] C. K. Ly, "SoftCopy display quality assurance program at Texas children's hospital," *J. Digit. Imag.*, vol. 15, no. s1, pp. 33–40, Mar. 2002.
[7] P. C. Brennan, M. McEntee, M. Evanoff, P. Phillips, W. T. O'Connor, and D. J. Manning, "Ambient lighting: Effect of illumination on soft-copy viewing of radiographs of the wrist," *Amer. J. Roentgenol.*, vol. 188, no. 2, pp. W177–W180, Feb. 2007.
[8] M. F. Mcentee, J. Ryan, M. G. Evanoff, A. Keeling, D. Chakraborty, D. Manning, and P. C. Brennan, "Ambient lighting: Setting international standards for the viewing of softcopy chest images," *Proc. SPIE*, vol. 6515, Mar. 2007, Art. no. 65150M.
[9] *Digital Imaging and Communications in Medicine (DICOM) Part 14: Grayscale Standard Display Function*, Nat. Elect. Manufacturers Assoc., Rosslyn, VI, USA, 2009.
[10] N. Tanaka, K. Naka, M. Sueoka, Y. Higashida, and J. Morishita, "Application of the grayscale standard display function to general purpose liquid-crystal display monitors for clinical use," *Jpn. J. Radiolog. Technol.*, vol. 66, no. 1, pp. 25–32, Jan. 2010.
[11] K. A. Fetterly, H. R. Blume, M. J. Flynn, and E. Samei, "Introduction to grayscale calibration and related aspects of medical imaging grade liquid crystal displays," *J. Digit. Imag.*, vol. 21, no. 2, pp. 193–207, Jun. 2008.
[12] *Digital Imaging and Communications in Medicine (DICOM)PS3. 3*, Nat. Elect. Manufacturers Assoc., Rosslyn, VI, USA, 2009.
[13] T. Kimpe, D. Deroo, and A. Xthona, "TU-EE-A3-05: Current challenges in DICOM GSDF calibration For medical displays," *Med. Phys.*, vol. 33, no. 6, p. 2209, 2006.
[14] P. G. J. Barten, *Contrast Sensitivity of the Human Eye and Its Effects on Image Quality*. Eindhoven, The Netherlands: Eindhoven University of Technology, 1999.
[15] P. G. J. Barten, "Physical model for the contrast sensitivity of the human eye," *Proc. SPIE*, vol. 1666, pp. 57–72, Aug. 1992.
[16] T. Oshika, C. Okamoto, T. Samejima, T. Tokunaga, and K. Miyata, "Contrast sensitivity function and ocular higher-order wavefront aberrations in normal human eyes," *Ophthalmology*, vol. 113, no. 10, pp. 1807–1812, Oct. 2006.
[17] D. L. Leong, L. Rainford, T. M. Haygood, G. J. Whitman, P. M. Tchou, W. R. Geiser, S. Carkaci, and P. C. Brennan, "Verification of DICOM GSDF in complex backgrounds," *J. Digit. Imag.*, vol. 25, no. 5, pp. 662–669, Oct. 2012.
[18] A. Liu, W. Lin, M. Paul, C. Deng, and F. Zhang, "Just noticeable difference for images with decomposition model for separating edge and textured regions," *IEEE Trans. Circuits Syst. Video Technol.*, vol. 20, no. 11, pp. 1648–1652, Nov. 2010.
[19] J. Yi, Q. Wang, D. Zhao, and J. T. Wen, "BP neural network prediction-based variable-period sampling approach for networked control systems," *Appl. Math. Comput.*, vol. 185, no. 2, pp. 976–988, Feb. 2007.
[20] S. Li, L. J. Liu, and Y. L. Xie, "Chaotic prediction for short-term traffic flow of optimized BP neural network based on genetic algorithm," *Control Decis.*, vol. 26, no. 10, pp. 1581–1585, Oct. 2011.
[21] W. Li, W. Li, C. Wang, Q. Wang, and G. Chen, "An edge detection method based on optimized BP neural network," in *Proc. Int. Symp. Inf. Sci. Eng.*, Dec. 2008, pp. 40–44.
[22] J. A. Rodger, "A fuzzy nearest neighbor neural network statistical model for predicting demand for natural gas and energy cost savings in public buildings," *Expert Syst. Appl.*, vol. 41, no. 4, pp. 1813–1829, Mar. 2014.
[23] K. Deb, A. Pratap, S. Agarwal, and T. Meyarivan, "A fast and elitist multiobjective genetic algorithm: NSGA-II," *IEEE Trans. Evol. Comput.*, vol. 6, no. 2, pp. 182–197, Apr. 2002.

ZILONG LIU received the Ph.D. degree from the Beijing Institute of Technology, Beijing, China, in 2013. He is currently an Associate Professor with the Optical Division, National Institute of Metrology, China. His research interests include high-dynamic optical imaging, optical sensors, and image processing technology.

YIQIN JIANG received the bachelor's degree from the Beijing University of Posts and Telecommunications. She is currently pursuing the master's degree in medical image metrology with the National Institute of Metrology (NIM), China.

YUXIAO LI was born in 1996. He received the bachelor's degree from the Beijing Institute of Technology, in 2018. He is currently with the National Institute of Metrology (NIM), China.

JIN LI was born in 1984. He is currently a Postdoctoral Fellow with the Department of Engineering, University of Cambridge, Cambridge, U.K. His research interests include high-dynamic optical imaging, optical sensors, and image processing technology.

ZHUORAN LI received the bachelor's degree from the Beijing University of Posts and Telecommunications, Beijing, China, in 2019. He is currently pursuing the master's degree with the Optical Division, National Institute of Metrology, China. His research interest includes image metrology.

SHUGUO ZHANG received the master's degree from Northwest University, Xi'an, China.

He is currently the Human Resources Manager of the State Grid Beijing Training Center.

YUSHENG LIAN received the Ph.D. degree from the Beijing Institute of Technology, Beijing, China, in 2014. He is currently an Associate Professor with the School of Printing and Packaging, Beijing Institute of Graphic Communication. His research interests include novel spectral imaging technology, color science and technology, and image processing technology.

RUPING LIU received the Ph.D. degree from the Institute of Electronics, Chinese Academy of Sciences, in 2010. She is currently an Associate Professor with the Beijing Institute of Graphic Communication. Her research interest includes neural microelectric signal process.